Elimination of Water from the Carboxyl Group of $GlyGlyH^+$

Bülent Balta and Viktorya Aviyente
Chemistry Department, Boğaziçi University, Istanbul, Turkey

Chava Lifshitz
Department of Physical Chemistry and the Farkas Center for Light Induced Processes, The Hebrew University of Jerusalem, Jerusalem, Israel

The elimination of water from the carboxyl group of protonated diglycine has been investigated by density functional theory calculations. The resulting structure is identical to the b_2 ion formed in the mass spectrometric fragmentation of protonated peptides (therefore named "b_2" in this study). The most stable geometry of the fragment ion ("b_2") is an O-protonated diketopiperazine. However, its formation is kinetically disfavored as it requires a free energy of 58.2 kcal/mol. The experimentally observed N-protonated oxazolone is 3.0 kcal/mol less stable. The lowest energy pathway for the formation of the "b_2" ion requires a free energy of 37.5 kcal/mol and involves the proton transfer from the amide oxygen of protonated diglycine to the hydroxyl oxygen. Fragmentation initiated by proton transfer from the terminal nitrogen has also a comparable free energy of activation (39.4 kcal/mol). Proton transfer initiating the fragmentation, from the highly basic terminal nitrogen or amide oxygen to the less basic hydroxyl oxygen is feasible at energies reached in usual mass spectrometric experiments. Amide N-protonated diglycine structures are precursors of mainly y_1 ions rather than "b_2" ions. In the lowest energy fragmentation channels, proton transfer to the hydroxylic oxygen, bond breaking and formation of an oxazolone ring occur concertedly but asynchronously. Proton transfer to hydroxyl oxygen and cleavage of the corresponding C–O bond take place at the early stages of the fragmentation step, while ring closure to form an oxazolone geometry occurs at the later stages of the transition. The experimentally observed low kinetic energy release is expected to be due to the existence of a strongly hydrogen bonded protonated oxazolone-water complex in the exit channel. Whereas the threshold energy for "b_2" ion formation (37.1 kcal/mol) is lower than for the y_1 ion (38.4 kcal/mol), the former requires a tight transition state with an activation entropy, $\Delta S^{\ddagger} = -1.2$ cal/mol.K and the latter has a loose transition state with $\Delta S^{\ddagger} = +8.8$ cal/mol.K. This leads to y_1 being the major fragment ion over a wide energy range. (J Am Soc Mass Spectrom 2003, 14, 1192–1203) © 2003 American Society for Mass Spectrometry

Mass spectrometry is an important tool for peptide and protein research as the fragmentation of protonated peptides and proteins gives information about their primary structure [1–4]. Amino acid sequence can be assigned by considering the fragments resulting from the cleavage of the peptide linkage, i.e., the b_n and y_n ions which are the N-terminal and C-terminal charged fragments respectively (the conventional nomenclature [5] of the ions is illustrated in the upper part of Scheme **1**).

According to the mobile proton model [6–9], the added proton can move along all basic sites before fragmentation occurs. When the added proton is situated on the amide oxygen atom, the peptide bond becomes stronger while protonation of the amide nitrogen weakens the peptide linkage and leads to fragmentation [10].

By comparison of the mass spectra of y_n ions with reference spectra, there exists clear evidence that the y_1 ions are protonated amino acids, similarly larger y_n ions are protonated peptides [11, 12]. On the other hand, using the neutral fragment reionization (N_fR) technique, it has been observed that when a b_n ion is produced, the C-terminus is cleaved as an intact amino acid (if the C-terminal amide bond is broken) or peptide (if an amide bond other than the C-terminal one is cleaved) [12].

The structure of the N-terminal ionic or neutral fragments is not clear. In early studies, the b_n ions have

Published online August 13, 2003

Supplementary material available: A complete documentation of the relative energies of all species and the dihedral angles defining the conformations are given as supplementary material (Tables S1–S9). To request a copy of the tables, please contact the JASMS editorial office in St. Louis, MO.

Address reprint requests to Dr. V. Aviyente, Chemistry Department, Boğaziçi University, Bebek, Instanbul, Turkey.

1044-0305/03/$30.00
doi:10.1016/S1044-0305(03)00479-3

Received December 31, 2002
Revised May 20, 2003
Accepted May 25, 2003

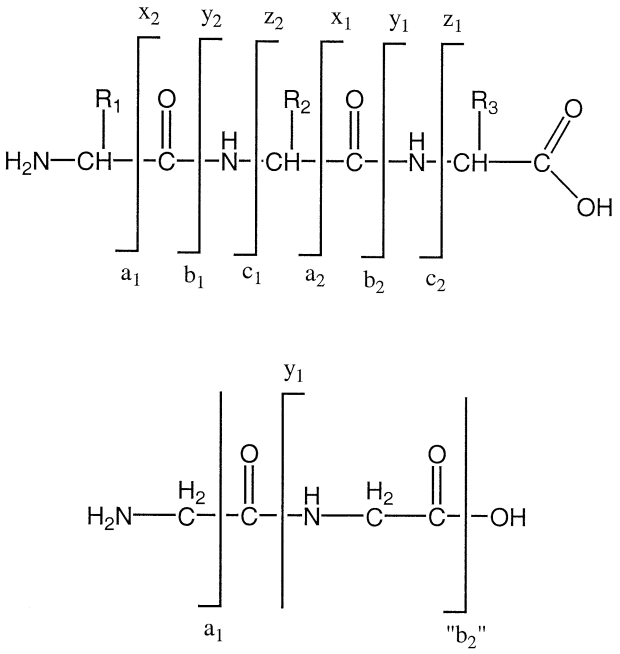

Scheme 1

been thought to be acylium ions (Scheme **2**) [1, 2, 4]. Later, it has been shown that the acylium ions are not stable and a N-protonated oxazolone structure (Scheme **2**) is proposed for b_n ions [13–20]. According to the oxazolone mechanism, the protonation of the amide bond causes a large positive charge on the amide carbon atom. Nucleophilic attack by the nearby amide carbonyl oxygen results in cyclization. The need for at least two amide bonds for this mechanism is consistent with the observation that amino acids other than the ones which can react with their own side chain do not form b_1 ions. On the other hand, N-acetylated amino acids are observed to give b_2 ions in their metastable ion and CID mass spectra [13]. A further evidence for the formation of a protonated oxazolone structure is that protonated 2-phenyl-5-oxazolone and the b_2 ion derived from N-benzoyl-Gly-Gly-OH produce identical mass spectra [13]. Moreover, the elimination of CO_2 from b_n ions is considered to be an indicator of an oxazolone structure [15]. The experimental findings are supported by ab initio calculations [8, 13, 14, 16, 20]. The protonated oxazolone may fragment further to an immonium ion (a_n ion) and carbon monoxide. Early calculations have indicated that the acyclic acylium ion is the transition state in the fragmentation of b_n ions to a_n species [13]. However, recent calculations have located an acyclic acylium ion as a very high energy local minimum (about 30 kcal/mol above the protonated oxazolone) [18].

The kinetic energy releases for the formation of b_2 ions from various peptides have been mesured as 0.02-0.03 eV, suggesting that no reverse activation barriers exist for these reactions [13].

Considering the relatively low proton affinity of the amide nitrogen, a mechanism consisting of protonation at the amide oxygen, yielding an O-protonated oxazolone structure (Scheme **2**), is also proposed [17]. However, the fragmentation of the b_2 ion from protonated diglycine occuring by the loss of CO and ab initio calculations indicating a higher stability for the N-protonated oxazolone (by 19.5 kcal/mol for oxazolones derived from protonated N-acetyl glycine) disagree with an O-protonated oxazolone structure [19].

Recently, carrying out DFT calculations, Rodriquez et al. [20] have found that the most favorable site of protonation on protonated triglycine is the carbonyl oxygen of the N-terminal residue. In the fragmentation process, a proton is transferred from the N-terminal carbonyl oxygen to the nitrogen atom of the leaving C-terminal residue, yielding a N-protonated oxazolone as the b_2 ion [20].

A protonated diketopiperazine structure (Scheme **2**) would form if the nitrogen atom of the nearby residue is involved in the nucleophilic attack to the amide carbon. However, comparison of the CID spectra of b_n ions with reference spectra gives strong evidence that cyclization to diketopiperazine does not occur [12, 13, 15]. On the other hand, N_fR experiments show that the neutral fragment lost during y_n formation has a diketopiperazine structure (except the case where only the N-terminal amino acid is lost) [12].

An immonium structure (Scheme **2**) is proposed by Eckart et al. for b_n ions in heteromeric sequences bearing the more basic residue at the N-terminus [21]. This idea has been opposed by Harrison and coworkers who have shown that Eckart's observations can be explained also by the oxazolone model [16].

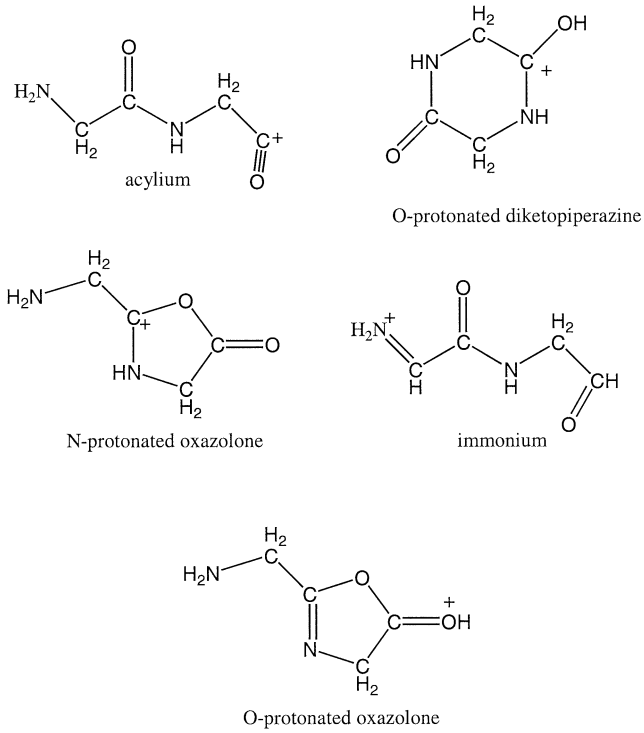

Scheme 2

Besides the structure of the b_n ion, the mechanism by which the extra proton is shuttled to the site of bond cleavage is of importance. Spatial proximity of the donor and acceptor sites as well as their proton affinities may direct the mobile proton to some locations, favoring the formation of certain fragment ions.

We have carried out calculations using density functional theory (DFT) on the simplest dipeptide diglycine to deduce the structure and formation mechanism of the b_2 ion. The reaction investigated in the present work, i.e., the elimination of water from the carboxyl group of protonated diglycine, does not involve the cleavage of the peptide linkage, nevertheless the resulting ionic fragment is identical to a b_2 ion. Therefore, throughout this paper, this ion will be named "b_2" and a nomenclature different than the conventional one will be used. The present nomenclature is illustrated in the lower part of Scheme **1**.

In CID experiments, Klassen and Kebarle have not observed the formation of "b_2" ion from protonated diglycine, the y_1 ion being the most abundant species at low collision energies and a_1 being the most abundant fragment at higher collision energies [22]. On the other hand, the CID experiments of Reid et al. have indicated the formation of the "b_2" ion, the most abundant fragment being the y_1 ion [19, 23]. Moreover, van Dongen et al. have found a significant "b_2" ion peak during the unimolecular decomposition of protonated diglycine [24].

The favored protonation site in diglycine is the terminal nitrogen [8, 25]. Paizs et al. have shown computationally that the proton can sample all basic sites before fragmentation occurs [8], in keeping with the mobile proton model [6, 7, 9]. They have proposed a mechanism that passes through an amide N-protonated species for the formation of the "b_2" ion. In this mechanism, proton transfer from the amide nitrogen to the hydroxyl group takes place concertedly with the cleavage of the C–O bond, bearing a transition state which is 44.8 kcal/mol above the most stable protonated diglycine structure on the electronic energy surface (including the zero point energy) [8]. The same authors have proposed also a mechanism for the integrated formation of the a_1 and y_1 ions passing through a transition state (corresponding to the breakdown of the amide N-protonated diglycine to immonium, carbon monoxide and neutral glycine) which is 38.4 kcal/mol above the most stable protonated diglycine structure [26]. The reaction yields either an a_1 ion together with carbon monoxide and neutral glycine or a y_1 ion accompanied by carbon monoxide and imine [26].

In the following, we examine the relative stabilities of the proposed structures for the "b_2" ion derived from protonated diglycine. Then, we show why the thermodynamically most stable O-protonated diketopiperazine structure is not detected experimentally. We investigate different channels resulting in N-protonated oxazolone, the most probable form of "b_2" based on experimental observations. We investigate the competition between the formation of "b_2" and y_1 ions by comparing our results with those of Paizs et al. [26].

Computational Methods

All the minimum energy structures and transition states have been fully optimized using the Becke-3-parameter-Lee-Yang-Parr exchange-correlation functional (B3LYP) [27, 28]. Previous calculations on the fragmentation of protonated monoglycine have yielded satisfactory results using this functional [29]. The 6-31 + G** basis set has been used in conjunction with the B3LYP method. This basis set is similar to the one we have used in the study of the fragmentation of protonated monoglycine (6-31 + G**) [29] except that diffuse functions on hydrogens are omitted in the present work. As the B3LYP method may be inadequate for proton transfer barriers, the global minimum, the highest energy transition state and the separated products in the lowest energy reaction channel, have been reoptimized at the MP2/6-31 + G** level of theory in order to confirm the B3LYP/6-31 + G** results. The MP2 and B3LYP results are in reasonable agreement. The results are further checked by MP4/6-31 + G** single point energy calculations using the MP2/6-31 + G** optimized geometries.

The nature of the stationary points has been checked by computing the harmonic vibrational frequencies. All real freaquencies have indicated the presence of global or local minima whereas one imaginary frequency has suggested a transition state. The fact that the located transition states connect the expected minima has been confirmed by intrinsic reaction coordinate (IRC) calculations.

E_{el}, E_{el+ZPE}, H_{298}, G_{298} and S_{298} refer to the electronic energy at 0 K, the sum of the electronic energy and zero point energy at 0 K, enthalpy at 298 K, Gibbs free energy at 298 K and entropy at 298 K, respectively. The zero point energies, entropies and thermal contributions to energy have been obtained from harmonic frequency calculations without scaling. A complete documentation of the relative energies of all species and the dihedral angles defining the conformations are given as supplementary materials (Tables S1–S9).

All the calculations have been performed using the Gaussian 98 program [30].

Some conclusions drawn regarding the geometry have been supported by a natural bond orbitals (NBO) analysis [31, 32]. The energetic contributions of electron delocalizations between two given NBOs are computed using the second order perturbation theory in the NBO context.

Results and Discussion

Relative Stabilities of the Proposed Structures for the "b_2" Ion from Protonated Diglycine

The geometries and relative stabilities of the O-protonated diketopiperazine (**b2a**), N-protonated oxazolone

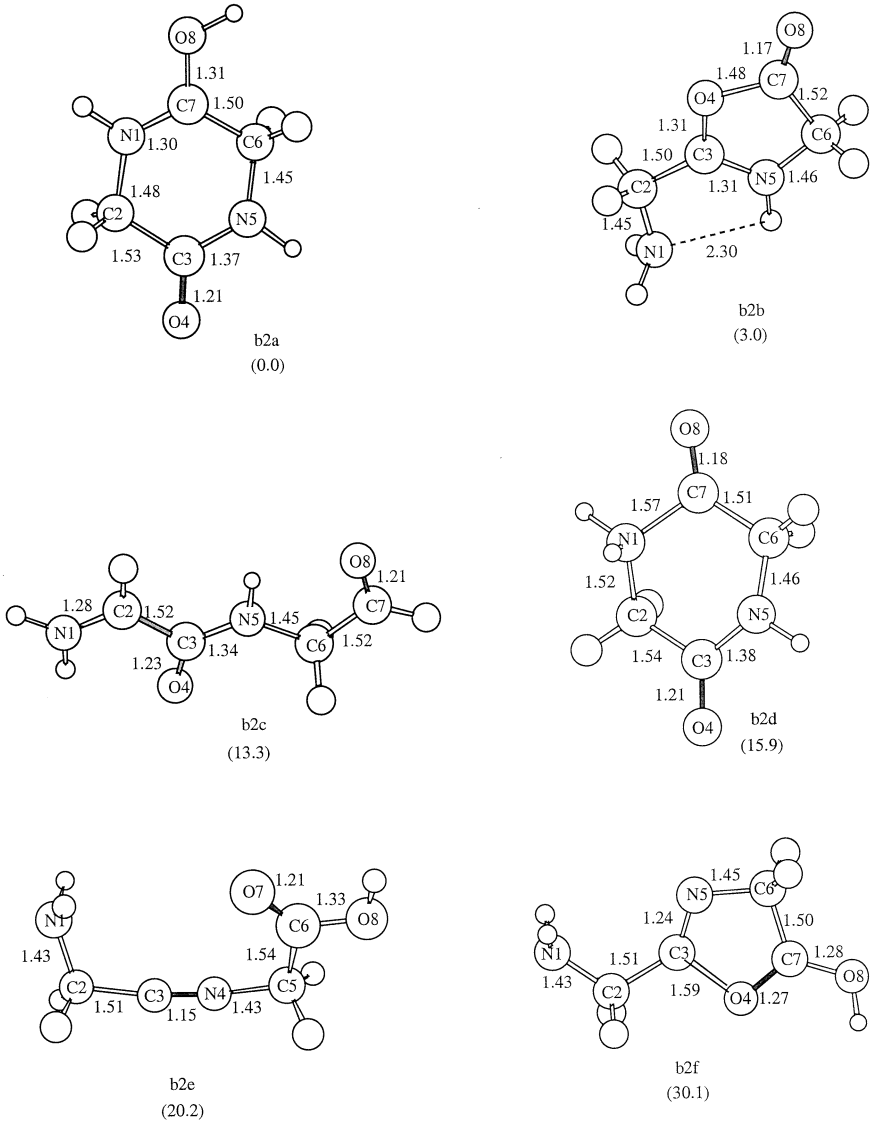

Figure 1. Ionic fragments resulting from the elimination of water. Bond lengths are in Å. The numbers in parentheses are the relative Gibbs free energies (in kcal/mol) with respect to **b2a**.

(**b2b**), immonium (**b2c**), N-protonated diketopiperazine (**b2d**) and O-protonated oxazolone (**b2f**) ions are displayed in Figure 1. The O-protonated diketopiperazine **b2a** is the most stable isomer. On a neutral diketopiperazine ring, conjugation in the amide group increases the proton affinity of the oxygen and decreases that of the nitrogen. Hence, the N-protonated diketopiperazine is significantly less stable than **b2a**.

The N-protonated oxazolone isomer (**b2b**) lies 3.0 kcal/mol above **b2a**. We have also tried to optimize O-protonated oxazolone structures. One such structure (**b2f**) has a very high energy and the C3–O4 bond is almost broken. Another starting geometry for an O-protonated oxazolone has ended up with a high energy structure (**b2e**) called a retro-Ritter product by Reid et al. [19], representing another way of water loss (from the amide oxygen) rather than forming a "b_2" ion.

The immonium ion **b2c** is less stable than **b2a** by a free energy of 13.3 kcal/mol. It must be noted that the calculations of Eckart et al., using the BLYP functional, have found that **b2c** and **b2b** are nearly isoenergetic and both are less stable than **b2a** by about 10 kcal/mol on the ΔE_{el} surface [21] (ΔE_{el} of **b2c** with respect to **b2a** is 16.0 in our calculations, and **b2b** is 12.4 kcal/mol more stable than **b2c**). This illustrates the importance of using hybrid DFT functionals instead of pure ones. The other calculations on dipeptides containing glycine and alanine, reported by Eckart et al. [21] involve relative energies that are within about 11 kcal/mol, i.e., less than the difference between BLYP and B3LYP results on the relative stabilities of **b2c** and **b2b**. Hence, it may be that these authors have been misled by the BLYP results when proposing that an immonium structure is more stable for "b_2" from Ala-Gly.

All our attempts to locate an acyclic acylium ion have resulted in a N-protonated oxazolone structure.

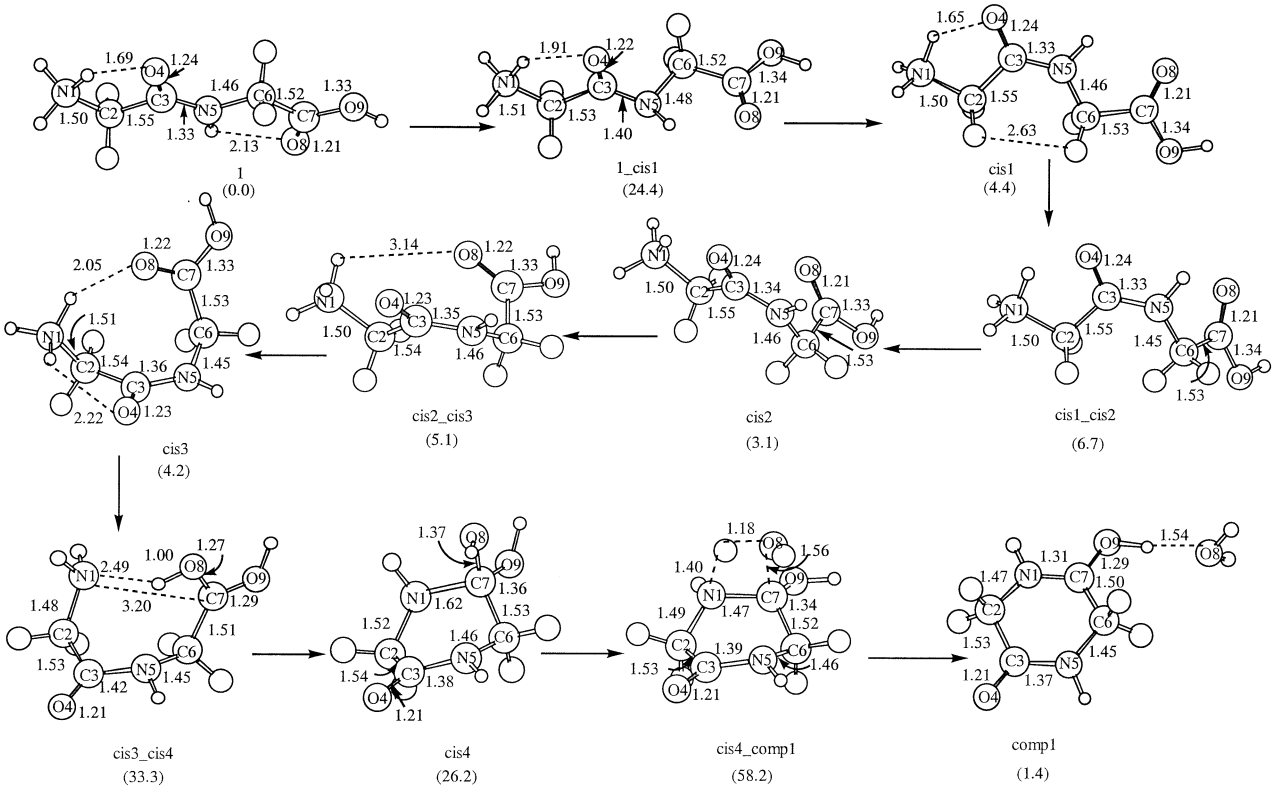

Figure 2. Structures involved in the formation of O-protonated diketopiperazine **b2a**. Bond lengths are in Å. The numbers in parentheses are the relative Gibbs free energies (in kcal/mol) with respect to **1**.

Why Does the O-Protonated Diketopiperazine Not Form?

The lowest energy pathway yielding an O-protonated diketopiperazine ion is depicted in Figure 2. Our calculations have located the terminal N-protonated diglycine **1** as the most stable parent ion structure, in agreement with the studies in the literature [8, 25]. The amide group in the diketopiperazine ring has a cis arrangements of the O-C-N-H atoms while in **1** the trans form is found. The diglycine isomers protonated at the amide nitrogen do not display a cis or trans arrangement as the peptide linkage has a single bond character. Hence, protonated diglycine isomers other than the ones protonated at the amide nitrogen have to undergo cis-trans isomerization before the ring closure leading to a diketopiperazine structure. Paizs et al. [33] have investigated the cis-trans isomerization around the amide bond in protonated triglycine, considering a pathway involving proton transfer from the N-terminal nitrogen to the neighboring amide nitrogen, rotation around the amide bond and back transfer of the proton to the N-terminal nitrogen. The highest energy transition state they have located, lies 20.1 kcal/mol above the most stable protonated triglycine structure on the ΔE_{el+ZPE} surface. On the other hand, in the present work, we have located a transition state for the cis-trans isomerization (**1_cis1**) which is 24.1 kcal/mol higher than the most stable diglycine structure **1** on the ΔE_{el+ZPE} surface. This transition state, connecting **1** and **cis1**, shows that cis-trans isomerization in protonated diglycine is feasible, even when the proton is situated on the terminal nitrogen leaving the amide bond with its partial double bond character. Thus, a considerable amount of cis isomers are expected to be found in mass spectrometric experiments below the threshold for fragmentation (see below for threshold energies in various fragmentation channels).

We have also considered alternative pathways for cis-trans isomerization. Cyclization to a diketopiperazine ring and elimination of water can occur concertedly starting from an amide N-protonated structure. The related transition state (ΔG_{298} = 50.9 kcal/mol) also includes contributions from the elimination of water and cyclization. We are not able to distinguish the contribution of the rotation around the amide bond to the barrier. The terminal N-protonated transition state, **1_cis1** has a relative free energy close to that of the amide N-protonated species (ΔG_{298} = 23.0 kcal/mol, see reference [8] for the relative energies of all amide N-protonated diglycines). Hence, the cis-trans isomerization does not necessarily involve amide N-protonated species.

The steric interactions between the methylene hydrogens of different residues destabilizes the cis isomer (the H. . .H distances are 2.63 Å). On the other hand, in **cis1** the N1-H. . .O4 hydrogen bond is stronger than the

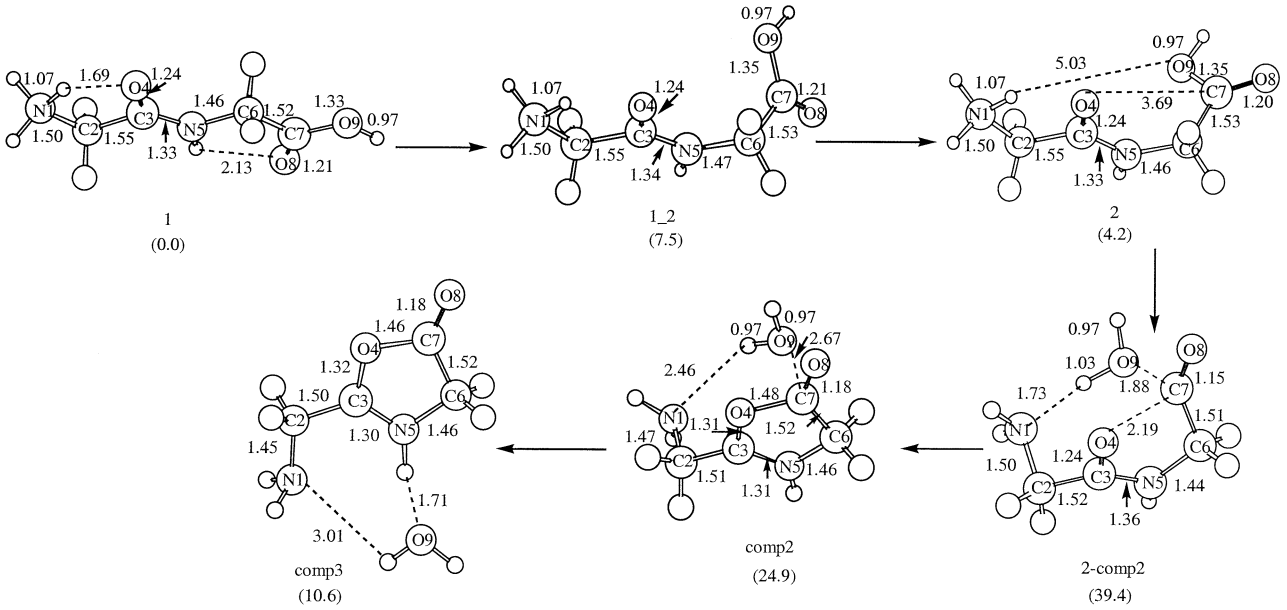

Figure 3. Structures involved in the formation of N-protonated oxazolone **b2b** via direct proton transfer from the terminal nitrogen. Bond lengths are in Å. The numbers in parentheses are the relative Gibbs free energies (in kcal/mol) with respect to **1**.

one in **1** shown by the corresponding hydrogen bond distance. The repulsive interactions between methylene hydrogens are partially compensated by the strength of this hydrogen bond to yield a rather low relative free energy for **cis1**. Species **cis1** converts to **cis2** and then **cis3** through low energy transition states. Rotations which lead to the loss or weakening of the intramolecular hydrogen bonds also lead to reductions in steric interactions by placing methylene hydrogens of different residues away from each other. Moreover, a new hydrogen bond (N1-H. . .O8) is formed in **cis3** and probably an electrostatic interaction (O8. . .C3) is present in **cis2**. Therefore, all cis species have very similar relative free energies and interconvert easily.

Proton transfer from N1 to O8 takes place in concert with cyclization. However, these processes are not synchronous. Proton transfer takes place before cyclization as shown by the geometry of the transition state **cis3_cis4**. Cyclization benefits from the creation of the positive charge on C7 upon proton transfer.

Starting with the cyclic species **cis4**, proton transfer from N1 and cleavage of the C7–O8 bond occurs concertedly through a four membered transition state, **cis4_comp1**. The resulting species, **comp1** is an O-protonated diketopiperazine-water complex which is only 1.4 kcal/mol higher in free energy than **1**. The low relative free energy of **comp1** is in part due to the intrinsic stability of the **b2a** moiety, but mostly to the tight hydrogen bond between **b2a** and water. The hydrogen bond free energy is 12.2 kcal/mol, computed as the difference between the relative free energies of **b2a** and separated products.

Instead of **cis3_cis4**, one may consider an alternative transition state in which the proton is transferred to O9, leading to the simultaneous formation of a N-protonated diketopiperazine and water (not shown in the figures). One such transition structure has a relative free energy of 50.9 kcal/mol (the proton is transferred from N5 and not from N1 but we do not expect that this fact changes the conclusions presented below). This transition state is lower than **cis4_comp1**, suggesting that the formation of **b2d** requires less energy than **b2a**, thus kinetically more favorable. From the resulting **b2d**-water complex, the water molecule evaporates. Then, **b2d** has to tautomerize to form the more stable **b2a**. The four membered transition state for tautomerization (not shown in the figures) has a relative free energy of 68.1 kcal/mol. In all cases, the free energy requirement for the formation of **b2a** is much higher than for **b2b**, preventing kinetically the formation of the most stable product.

Formation of the N-Protonated Oxazolone

Direct proton transfer from the terminal nitrogen. In order for fragmentation to occur, the ionizing proton has to migrate to the hydroxyl oxygen of the protonated diglycine. Starting from **1**, the simplest route is the direct proton transfer from the terminal nitrogen to the hydroxyl oxygen. The geometries of the species involved in this reaction channel are displayed in Figure 3.

The transition state **1_2** converts the most stable species **1** to **2** through coupled rotations around the N5–C6 and C6–C7 bonds. The rotamer **2** still displays the N1-H. . .O4 hydrogen bond while the conformational rearrangement leads to the loss of the N5-H. . .O8 hydrogen bond which is compensated to some extent by an electrostatic interaction between C3 and O9.

Along the reaction coordinate from **2** to **comp2**, rotation around the C2–C3 bond occurs first, allowing the proton to come closer to O9. Then, the proton transfer from N1 to O9 accompanied by the breaking of the C7–O9 bond takes place. At the transition state **2_comp2**, the water molecule is already formed and connected to the rest of the system by a charge transfer interaction at C7 (the charge transfer energies from one of the lone pairs of O9 into the two antibonding orbitals on the C7–O8 bond are 38.2 and 32.9 kcal/mol) and a hydrogen bond at N1, rather than covalent bonds as demonstrated by the long C7. . .O9 and N1. . .H distances. A charge transfer interaction between one of the O4 lone pairs and the two antibonding orbitals on the C7–O8 bond is detected (contributing 7.7 and 10.6 kcal/mol). The amide bond in **2_comp2** is substantially long and distorted from planarity (by 24.9°). For comparison, the highest energy point along the fragmentation pathway of protonated monoglycine via direct proton transfer from nitrogen to the hydroxylic oxygen on the ΔE_{el+ZPE} surface is about 35 kcal/mol (the final products are an immonium ion, carbon monoxide and water) [34].

The ring closure occurs after the transition state and a protonated oxazolone-water complex **comp2** is formed. The N1-C2-C3-N5 dihedral angle of −83.8° disables the intramolecular hydrogen bond N1. . .H-N5 encountered in **b2b**. Hence, the complex has a high relative free energy. The oxygen O9 interacts with C7 from a long distance, yielding a charge transfer energy of 3.3 kcal/mol. Similarly, one of the water hydrogens interacts weakly with N1 from a distance of 2.46 Å with a charge transfer energy of 2.9 kcal/mol. The low degree of charge transfer reveals that **comp2** is mainly an electrostatically held ion-dipole complex.

The weakly bound ion-dipole complex **comp2** rearranges to the substantially more stable hydrogen bonded complex **comp3**. The glycine moiety in **comp3** is similar to **b2b**. The water molecule is hydrogen bonded to the formerly amide proton. We have not been able to locate a transition state between **comp2** and **comp3**. Nevertheless, we expect that a transition state involving the migration of a weakly held water molecule and rotation around the C2–C3 bond is not too high in free energy relative to **comp2**.

The separated products, i.e., **b2b** and water lie 6.0 kcal/mol above **comp3** on the ΔG_{298} surface. The presence of this complex, in the exit channel, which is lower in free energy than the separated products explains the experimentally observed low kinetic energy release [13].

The pathway presented above requires less energy than the one proposed by Paizs et al. (37.9 versus 44.8 on the ΔE_{el+ZPE} surface) [8]. Moreover, no high energy amide N-protonated species are involved. It is clear that proton transfer from the most basic site (terminal nitrogen) to the least basic site (hydroxyl oxygen) is feasible at energies reached in usual mass spectrometric experiments, provided that the proton donor and acceptor get close to each other in space (no matter how they are far apart on the amino acid sequence).

Direct proton transfer from the amide oxygen. Due to the conjugation along the amide bond, the amide oxygen is a good nucleophile. Hence, proton shuttle from the most basic terminal nitrogen to the hydroxyl oxygen through the amide oxygen is expected to be favorable at least thermodynamically. The geometries of the species involved in this pathway are presented in Figure 4.

The O-protonated isomer **3** is very close in energy to **1**. The stability of this isomer comes from the strong hydrogen bond between N1. . .H-O4. Interestingly, the O-protonated monoglycines have been found to be 15.8–30.8 kcal/mol less stable than the most stable N-protonated isomer at the B3LYP/6-31++G** level of theory [29]. The transition state **1_3** has an extremely low free energy. It may be assumed that the two minima are physically indistinguishable and the proton oscillates between the two basic sites.

Rotation around C6–C7 coupled with a rotation around N5–C6 occurs through the transition state **3_4**. The resulting local minimum **4** is the O-protonated analog of **2**. The transition state **4_5** consists of a series of internal rotations. The loss of the intramolecular hydrogen bond and the partial double bond character of the C3–O4 bond renders the rotation around the C3–O4 bond energy demanding. The rotations around N5–C6 and C6–C7 bring the hydroxyl oxygen O9 close to the proton attached to O4 (2.36 Å). Meanwhile, rotation around the C2–C3 bond moves N1 far apart from O4 which begins to orient its lone pairs towards the N-terminus. Due to the rotation around the C2–C3 bond, the repulsive interaction between the lone pairs of N1 and O4 is avoided.

The O-protonated conformer **5** is a relatively high energy structure because the N-terminal amino group is not hydrogen bonded. The O4-H. . .O9 hydrogen bond forming a seven membered ring in **5** is expected to be weaker than the O4-H. . .N1 hydrogen bond in **3** and **4**. The relatively less stable **5** easily converts to **6** in which the N-terminal amino group is involved in N1. . .H-N5 hydrogen bonding.

The transition from **6** to **comp4** consists of a concerted proton transfer from O4 to O9 and the cleavage of the C7–O9 bond. At the transition state **6_comp4**, the water molecule is already formed and has started to leave the remaining ion as in **2_comp2**. Similarly, the water molecule is held by a hydrogen bond with O4 and a charge transfer interaction between O9 and C7. The C7. . .O9 interaction has a very high covalent character (delocalizations from O9 to the C7–O8 antibonding orbitals give 91.2 and 24.0 kcal/mol). Cyclization to form the oxazolone ring is not advanced in **6_comp4** (the O4. . .C7 distance is 2.35 Å), nevertheless charge transfer energies of 10.0 and 7.7 kcal/mol between one of O4 lone pairs and the C7–O8 antibonding orbitals are detected.

The complex formed after cyclization, **comp4**, dis-

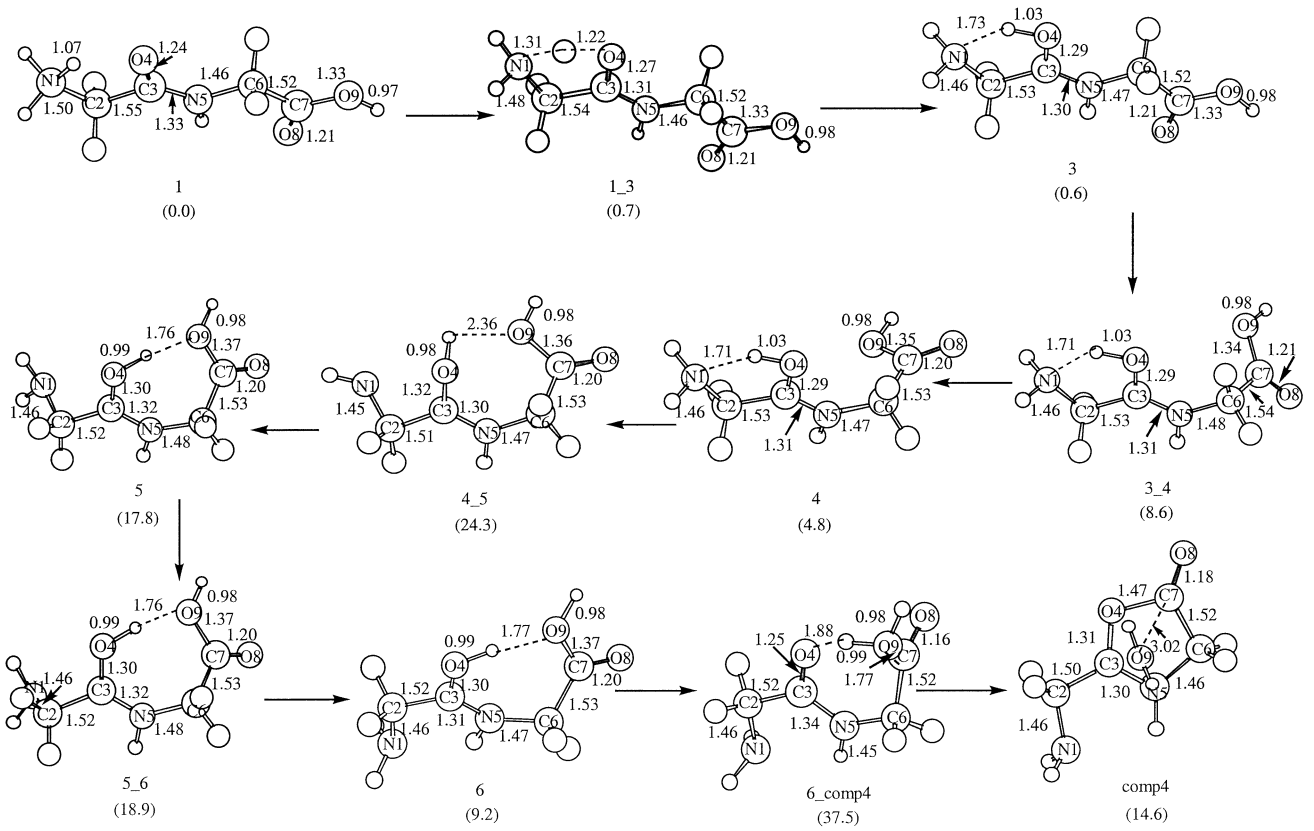

Figure 4. Structures involved in the formation of N-protonated oxazolone **b2b** via direct proton transfer from the amide oxygen. Bond lengths are in Å. The numbers in parentheses are the relative Gibbs free energies (in kcal/mol) with respect to **1**.

plays a N1. . .H-N5 hydrogen bond in contrast to **comp2**. No important charge transfer is observed between water and the "b_2" ion, indicating that **comp4** is mainly an ion-dipole complex. As **comp2**, **comp4** rearranges to the more stable hydrogen bonded complex **comp3**. We have not been able to locate any transition state for this rearrangement. Finally, **comp3** dissociates with a low kinetic energy release.

The highest energy structure in the above mechanism, **6_comp4**, is lower than **2_comp2** by 1.8 kcal/mol. Hence, the formation of the "b_2" ion from protonated diglycine is expected to occur mainly through the mechanism involving protonation of the amide oxygen, while the other mechanism may compete with it.

The sequence **4** → **4_5** → **5** → **5_6** → **6** involves a conformational rearrangement of the N-terminal amino group along the C2–C3 bond (besides the rotation around C3–O4 bond). Such a rotation may not be feasible in a long peptide far from the termini or a conformation in which N1 and O4 are syn to each other may be more stable than conformations bearing an anti orientation of these atoms. Hence, in order to compare the energetics of the fragmentation reaction starting with different reactive conformations, we have optimized the O-protonated parent ion, transition state of the fragmentation and the final complex with a syn arrangement of N1 and O4. The geometries are given in Figure 5. Of course, in a large peptide, the hydroxyl group present in diglycine will be replaced by an amino acid or a peptide. These groups are more basic than water and will lower the proton transfer barrier. Also, amide N-protonated species are stable, hence the proton transfer and fragmentation will not be concerted. Keeping in mind all these differences, our aim below, is to explore the effect of the conformation around the C2–C3 bond on the energetics of the reaction.

Although the bond lengths and interaction distances are slightly different, the reactive region of **7**, **comp5**, and **7_comp5** display similar features as **6**, **comp4**, and **6_comp4**, respectively, i.e., there is a seven membered ring in the reactant, the water molecule is already formed whereas cyclization is not observed in the transition state and the product is a complex of water and N-protonated oxazolone. The structures **7**, **7_comp5**, and **comp5** are 7–9 kcal/mol less stable than **6**, **6_comp4**, and **comp4**. Nevertheless, the free energy of the transition state with respect to the minima it connects is reasonably close in both reactions. The conformational change increases the relative energy of all stationary points approximately by the same amount due to the absence of a hydrogen bond in a spectator region of the system, but does not induce significant effects on the reactive region.

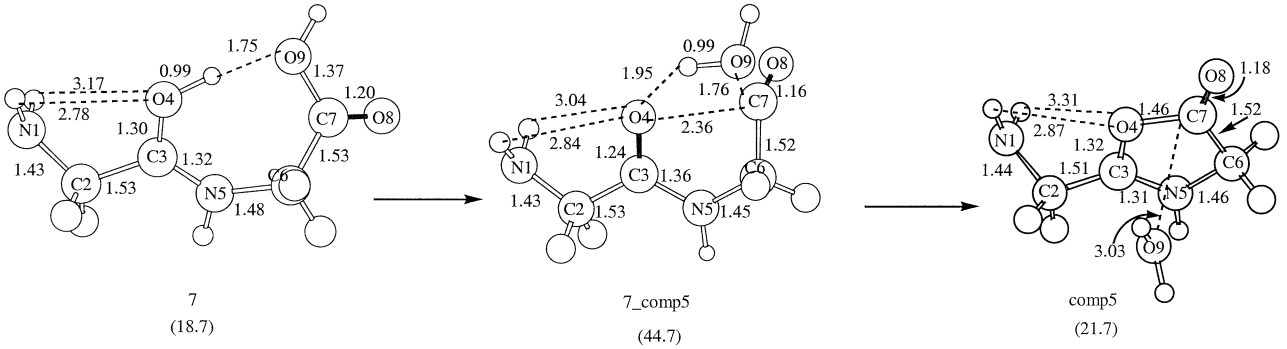

Figure 5. The transition state and corresponding minima involved in the formation of N-protonated oxazolone **b2b** via direct proton transfer from the amide oxygen when the terminal nitrogen and amide oxygen are in a syn arrangement. Bond lengths are in Å. The numbers in parantheses are the relative Gibbs free energies (in kcal/mol) with respect to **1**.

Proton transfer from the amide nitrogen. The elimination of water initiated by a proton transfer from amide nitrogen to O9 has been already modeled by Paizs et al. at the B3LYP/6-31G* level of theory [8] and the stability of each species involved in this reaction channel has been discussed [8]. We have simply reoptimized the structures reported by this group [8] at the B3LYP/6-31 + G** level of theory in order to make a better comparison with the energetics of the mechanisms discussed above. The geometries are displayed in Figure 6.

The initial conformational rearrangement (leading to **2**) is the same as the one in the mechanism initiated by direct proton transfer from N1 to O9. Also, the final complex is **comp4** (actually its mirror image as displayed in Figure 6). The energy requirement of the proton transfer from N1 to N5 is comparable to the conformational rearrangement barrier **4_5** in the mechanism passing through amide O-protonated species. The relative energy of the amide N-protonated **8** and the activation energy for its formation are well below the activation energy of the fragmentation steps. Therefore, a considerable amount of amide N-protonated species can exist. On the other hand, the transition state **8_comp4** is higher in energy than the ones in the other mechanisms discussed above. Moreover, the cleavage of the amide bond, which involves amide N-protonated structures, requires less energy ($\Delta E^{\ddagger}_{el+ZPE}$ = 38.4 kcal/mol) [26] than **8_comp4**. Hence, we think that amide N-protonated species do not play an important role in the formation of the "b_2" ion from protonated diglycine, rather they are intermediates for the formation of y_1 and a_1 ions.

Proton transfer from the terminal carbonyl oxygen. We have not been able to locate any open chain terminal carbonyl O-protonated species, in agreement with the findings of Paizs et al. [8]. In protonated trans diglycines, proton transfer to the terminal carbonyl oxygen occurs always in concert with a nucleophilic attack by the amide oxygen to the terminal carboxyl carbon, leading to a five membered ring carrying a geminal diol functionality. The barrier for this transition ($\Delta G^{\ddagger}_{298}$ =

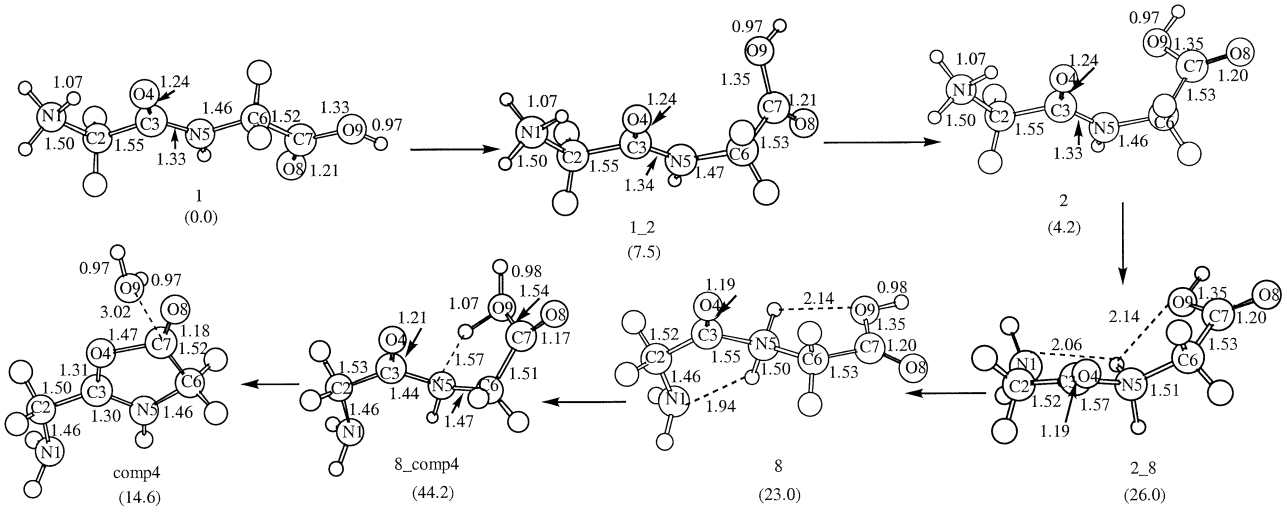

Figure 6. Structures involved in the formation of N-protonated oxazolone **b2b** via direct proton transfer from the amide nitrogen. Bond lengths are in Å. The numbers in parantheses are the relative Gibbs free energies (in kcal/mol) with respect to **1**.

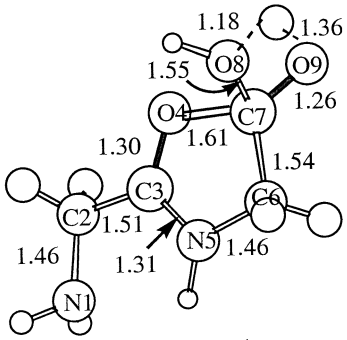

9_comp4
(59.4)

Figure 7. Transition state for the proton transfer between the carboxylic oxygens and elimination of water. Bond lengths are in Å. The number in parenthesis is the relative Gibbs free energy (in kcal/mol) with respect to **1**.

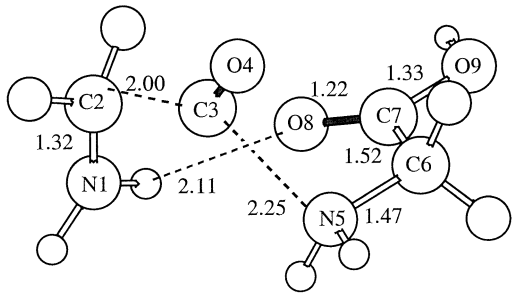

tsy1
(36.8)

Figure 8. Transition state for the simultaneous formation of glycine, carbon monoxide and immonium ion along the pathway for the formation of a_1 and y_1 ions. Bond lengths are in Å. The number in parenthesis is the relative Gibbs free energy (in kcal/mol) with respect to **1**.

25.7 kcal/mol) is comparable to the conformational rearrangement barrier **4_5** and the proton transfer barrier from N1 to N5, **2_8**. Hence, a considerable amount of terminal carbonyl O-protonated cyclic geminal diol species can exist. However, as already noted by Paizs et al. [8], the transition state for the proton transfer between the oxygens of the geminal diol group has a relative free energy of 59.4 kcal/mol. This transition state, **9_comp4**, is depicted in Figure 7. This high barrier suggests that such a fragmentation channel may be open only at high collision energies in CID experiments. It is also interesting to note that in protonated monoglycine, the barrier for proton transfer in the geminal diol group is much higher ($\Delta E^{\ddagger}_{el+ZPE}$ = 71.6 kcal/mol) [29].

Competition between the formation of b_n and y_n ions. Although N_fR experiments suggest that the formation of y_n ions in peptides with n + 1 amino acid residues, proceeds via the elimination of a neutral aziridinone [12], DFT calculations of Paizs et al. [26] show that the lowest energy path yielding y_1 from protonated diglycine passes through a transition state (E_{el+ZPE} = 38.4 kcal/mol) yielding a complex of an immonium ion, carbon monoxide and glycine concertedly. Carbon monoxide is easily evaporated from the complex if an internal energy of 1–2 kcal/mol is supplied [26]. Subsequent proton transfer in the remaining bimolecular complex leads to the formation of y_1 and an imine [26]. We have optimized several transition states yielding an aziridinone ring, however all of them are significantly higher in free energy than **tsy1**. We have also looked for transition states leading to acyclic neutral fragments, but we have not found any. Therefore, we have considered **tsy1** as the transition state leading to y_1. We have computed the relative free energies and entropies of the transition state (**tsy1**, Figure 8) and final products reported by Paizs et al. [26] as entropy effects are important. The relative energies of the highest energy transition states involved in different pathways of "b_2" and y_1 formation, their activation entropies as well as the relative energies of the final products are given in Table 1.

The lowest energy transition state for the formation of the "b_2" ion, **6_comp4**, is very close in free energy to **tsy1** at the B3LYP/6-31 + G** level of theory. Assuming that thermal corrections and entropy effects are similar at the different computational methods used here (only E_{el} has been computed with MP2 and MP4 as these

Table 1. The relative electronic energies (ΔE_{el}), sum of the electronic and zero point energies (ΔE_{el+ZPE}), enthalpies at 298 K (ΔH_{298}), Gibbs free energies at 298 K (ΔG_{298}) of the highest energy transition states and final product in each reaction channel with respect to the most stable parent ion 1, computed at the B3LYP/6-31 + G** level of theory. All energy values are in kcal/mol; entropies are in cal/mol.K.

	ΔE_{el}	$\Delta E_{el\ +\ ZPE}$	ΔH_{298}	ΔG_{298}	ΔS_{298}
1	0.0 (0.0)[a] [0.0][b]	0.0	0.0	0.0	0.0
cis4_comp1	59.0	56.1	55.2	58.2	−10.1
b2a+water	26.1	22.3	23.3	13.6	32.4
2_comp2	40.0	37.9	37.5	39.4	−6.2
6_comp4	39.7 (37.0) [35.5]	37.1	37.2	37.5	−1.2
7_comp5	47.6	44.6	44.9	44.7	0.7
8_comp4	47.6	44.0	43.9	44.2	−0.9
9_comp4	62.4	58.3	57.9	59.4	−4.8
b2b + water	29.8 (29.9) [29.2]	25.2	26.3	16.6	32.5
tsy1	41.9 (42.5) [37.8]	38.4	39.4	36.8	8.8
imine + CO + y_1	52.8 (50.2) [44.9]	46.2	48.2	24.7	78.8

[a]The numbers in parentheses are the relative electronic energies from the MP2/6 − 31 + G** optimizations.
[b]The numbers in square brackets are from the MP4/6− 31 + G** single point calculations based on the MP2/6 − 31 + G** geometries.

methods require too much computational resources), **tsy1** and **6_comp4** have again very close ΔG_{298} values with MP2 and MP4. Experimentally, the y_1 ion has been found to be more abundant than "b_2" [19, 23, 24]. Moreover, in the CID spectrum of protonated diglycine there are significant peaks due to the CO and (CO, NH_3) eliminations [19, 23]. According to the mechanism proposed by Reid et al. [23] these reactions also proceed via a transition state in which the parent ion fragments into three pieces. Paizs et al. argue that the elimination of CO occurs through **tsy1** [26].

There are two major reasons for the low abundance of the "b_2" ion: (1) The internal energy window in which it can be formed is very narrow: 37.1–38.4 kcal/mol (Table 1). Above the threshold of y_1 formation (ΔE_{el+ZPE} = 38.4 kcal/mol) the latter ion becomes the dominant product because it has a very loose transition state. (2) There are very large kinetic and competitive shifts for all the reactions of protonated diglycine [22]. As a result, dissociation over the energy range over which "b_2" is dominant is further suppressed.

Conclusion

The elimination of water from the terminal carboxyl group of protonated diglycine has been probed using B3LYP/6-31 + G** calculations. The relative stabilities of the proposed structures for the resulting ion (named "b_2" here) have been computed. The O-protonated diketopiperazine structure has been found to be the most stable one, while the N-protonated oxazolone lies 3.0 kcal/mol above. However, the formation of the O-protonated diketopiperazine is kinetically disfavored. The other proposed structures are 13–30 kcal/mol less stable. No linear acylium structure could be located.

The formation of water and oxazolone ring happen concertedly during fragmentation. In the early stages of the fragmentation step, proton transfer to the hydroxyl oxygen accompanied with the cleavage of the corresponding C–O bond occurs. In the final stage of the fragmentation, the ring closure yielding an oxazolone structure takes place (except the terminal carbonyl O-protonated species which bears already a ring structure).

The lowest energy channel for fragmentation involves the transfer of the proton from the amide oxygen to the site of bond breaking. Fragmentation triggered by proton transfer from the terminal nitrogen to the hydroxyl oxygen requires slightly more energy. Fragmentation mechanisms initiated by proton transfer from amide nitrogen and especially from terminal carbonyl oxygen require higher internal energies. Once the reactive conformations are formed, proton transfer from the highly basic terminal nitrogen or amide oxygen to the less basic hydroxyl oxygen is more feasible than proton transfer from other basic sites to the hydroxyl oxygen.

Amide N-protonated species can pass through the transition state for y_1 formation more easily than the one for "b_2" formation. Hence, they are expected to be precursors of mainly y_1 rather than "b_2" ions.

The formation of "b_2" and y_1 occurs via two competing reaction channels. However, "b_2" is the major ion over a very limited range of internal energies in the protonated diglycine ion—between 37.1 and 38.4 kcal/mol. Once the energy threshold for y_1 is exceeded, it becomes the favored reaction channel since it has a much looser transition state than "b_2" formation ($\Delta S(y_1)^{\ddagger}$ = +8.8 cal/mol.K vs. $\Delta S(\text{"}b_2\text{"})^{\ddagger}$ = −1.2 cal/mol.K). Indeed, in threshold CID measurements, "b_2" ions have not been reported at all [22]. Energy resolved breakdown curves [19] have indicated that "b_2" has a lower energy threshold than y_1 but the latter is the dominant ion at higher collision energies and reaches much higher overall intensities. These results have now been clarified through our calculations of the activation entropies for the two competing channels. Our implicit assumption is that the competition between the two reaction channels is controlled by the transition states **tsy1** and **6_comp4**. The RRKM expression for k(E) for the "b_2" formation is controlled by the density of states of the deepest potential well-structure **1**, and the sum of states is that of the transition state **6_comp4** (Figure 4). It is predicted that eventually more elaborate RRKM calculations of the rate energy dependencies, k(E) and of breakdown graphs as a function of internal energy in the precursor will verify this behavior.

The experimentally observed low kinetic energy release in the formation of the "b_2" ion is found to be due to the presence of a low energy hydrogen bonded complex in the exit channel.

Acknowledgments

The authors thank the Boğaziçi Üniversitesi Arastirma Fonu for support through project 01HB502D. The Farkas Research Center is supported by the Minerva Gesellschaft für die Forschung GmbH, München, Germany.

References

1. Biemann, K.; Martin, S. A. Mass Spectrometric Determination of the Amino Acid Sequence of Peptides and Proteins. *Mass Spectrom. Rev.* **1987,** *6,* 1–76.
2. Biemann, K. Sequencing of Peptides by Tandem Mass Spectrometry and High-Energy Collision Induced Dissociation. In: McCloskey, J. A., Ed.; *Mass Spectrometry, Methods in Enzymology, 193.* Academic Press: San Diego, 1990; 455–479.
3. Biemann, K. Primary Studies of Peptides and Proteins. *Biological Mass Spectrometry: Present and Future;* In: Matsuo, T.; Caprioli, R. M.; Gross, M. L.; Seyama, Y., Eds.; Wiley: New York, 1993; 275–297.
4. Papayannopoulos, I. A. The Interpretation of Collision-Induced Dissociation Tandem Mass Spectra of Peptides. *Mass Spectrom. Rev.* **1995,** *14,* 49–73.
5. Roepstorff, P.; Fohlman, J. Proposal for a Common Nomenclature for Sequence Ions in Mass Spectra of Peptides. *Biomed. Mass Spectrom.* **1984,** *11,* 601.
6. Tsang, C. W.; Harrison, A. G. Chemical Ionization of Amino Acids. *J. Am. Chem. Soc.* **1976,** *98,* 1301–1308.

7. Harrison, A. G.; Yalcin, T. Proton Mobility in Protonated Amino Acids and Peptides. *Int. J. Mass Spectrom. Ion Processes* **1997,** *165/166,* 339–347.
8. Paizs, B.; Csonka, I. P.; Lendvay, G.; Suhai, S. Proton Mobility in Protonated Glycylglycine and N-Formylglycylglycinamide: A Combined Quantum Chemical and RRKM Study. *Rapid Commun. Mass Spectrom.* **2001,** *15,* 637–650.
9. Dongré, A. R.; Jones, J. L.; Somogyi, A.; Wysocki, V. H. Influence of Peptide Composition , Gas-Phase Basicity, and Chemical Modification on Fragmentation Efficiency: Evidence for the Mobile Proton Model. *J. Am. Chem. Soc.* **1996,** *118,* 8365–8374.
10. Somogyi, A.; Wysocki, V. H.; Mayer, I. The Effect of Protonation Site on Bond Strengths in Simple Peptides: Application of ab initio and Modified Neglect of Differential Overlap Bond Order and Modified Neglect of Differential Overlap Energy Partitioning. *J. Am. Soc. Mass Spectrom.* **1994,** *5,* 704–717.
11. Mueller, D. R.; Eckersley, M.; Richter, W. Hydrogen Transfer Reactions in the Formation of "y + 2" Sequence Ions from Protonated Peptides. *Org. Mass Spectrom.* **1988,** *23,* 217–222.
12. Cordero, M. M.; Houser, J. J. Wesdemiotis C. The Neutral Products Formed During Backbone Fragmentation of Protonated Peptides in Tandem Mass Spectrometry. *Anal. Chem.* **1993,** *65,* 1594–1601.
13. Yalcin, T.; Khouw, C.; Csizmadia, I. G.; Peterson, M. R.; Harrison, A. G. Why are B Ions Stable Species in Peptide Spectra? *J. Am. Soc. Mass Spectrom.* **1995,** *6,* 1165–1174.
14. Yalcin, T.; Csizmadia, I. G.; Peterson, M. R.; Harrison, A. G. The Structure and Fragmentation of B_n ($n \geq 3$) Ions in Peptide Spectra. *J. Am. Soc. Mass Spectrom.* **1996,** *7,* 233–242.
15. Nold, M. J.; Wesdemiotis, C.; Yalcin, T.; Harrison, A. G. Amide Bond Dissociation in Protonated Peptides. Structures of the N-Terminal Ionic and Neutral Fragments. *Int. J. Mass Spectrom. Ion Processes* **1997,** *164,* 137–153.
16. Harrison, A. G.; Csizmadia, I. G.; Tang, T. H. Structure and Fragmentation of b_2 Ions in Peptide Mass Spectra. *J. Am. Soc. Mass Spectrom.* **2000,** *11,* 427–436.
17. Arnot, D.; Kottmeier, D.; Yates, N.; Shabanowitz, J.; Hunt, D. F. *Fragmentation of Multiply Protonated Peptides Under Low Energy Conditions.* Proceedings of the 42nd ASMS Conference on Mass Spectrometry and Allied Topics: Chicago, IL, June, 1994; p. 470.
18. Paizs, B.; Szlávik, Z.; Lendvay, G.; Vékey, K.; Suhai, S. Formation of a_2^+ Ions of Protonated Peptides. An ab initio Study. *Rapid Commun. Mass Spectrom.* **2000,** *14,* 746–755.
19. Reid, E. G.; Simpson, R. J.; O'Hair, R. A. J. A Mass Spectrometric and ab initio Study of the Pathways for Dehydration of Simple Glycine and Cysteine-Containing Peptide $[M + H]^+$ Ions. *J. Am. Soc. Mass Spectrom.* **1998,** *9,* 945–956.
20. Rodriquez, C. F.; Cunje, A.; Shoeib, T.; Chu, I. K.; Hopkinson, A. C.; Siu, K. W. M. Proton Migration and Tautomerism in Protonated Triglycine. *J. Am. Chem. Soc.* **2001,** *123,* 3006–3012.
21. Eckart, K.; Holthausen, M. C.; Koch, W.; Spiess, J. Mass Spectrometric and Quantum Mechanical Analysis of Gas-Phase Formation, Structure, and Decomposition of Various b_2 Ions and Their Specifically Deuterated Analogs. *J. Am. Soc. Mass Spectrom.* **1998,** *9,* 1002–1001.
22. Klassen, J. S.; Kebarle, P. Collision-Induced Dissociation Threshold Energies of Protonated Glycine, Glycinamide, and Some Related Small Peptides and Peptide Amino Amides. *J. Am. Chem. Soc.* **1997,** *119,* 6552–6563.
23. Reid, E. G.; Simpson, R. J.; O'Hair, R. A. J. Probing the Fragmentation Reactions of Protonated Glycine Oligomers via Multistage Mass Spectrometry and Gas Phase Ion Molecule Hydrogen/Deuterium Exchange. *Int. J. Mass Spectrom.* **1991,** *190/191,* 209–230.
24. van Dongen, W. D.; Heerma, W.; Haverkamp, J.; de Koster, C. G. The B_1 Fragment Ion from Protonated Glycine is an Electrostatically-bound Ion/Molecule Complex of CH_2–NH_2^+ and CO. *Rapid Commun Mass Spectrom.* **1996,** *10,* 1237–1239.
25. Zhang, K.; Zimmerman, D. M.; Chung-Phillips, A.; Cassady, C. J. Exprimental and ab initio Studies of the Gas-Phase Basicities of Polyglycines. *J. Am. Chem. Soc.* **1993,** *115,* 10812–10822.
26. Paizs, B.; Suhai, S. Theoretical Study of the Main Fragmentation Pathways for Protonated Glycylglycine. *Rapid Commun. Mass Spectrom.* **2001,** *15,* 651–663.
27. Becke, A. D. Density Functional Thermochemistry. III. The Role of Exact Exchange. *J. Chem. Phys.* **1993,** *98,* 5648–5652.
28. Lee, C.; Yang, W.; Parr, R. G. Development of Colle-Salvetti Correlation Energy Formula into a Functional of the Electron Density. *Phys. Rev. B* **1988,** *37,* 785–789.
29. Balta, B.; Basma, M.; Aviyente, V.; Zhu, C.; Lifshitz, C. Structures and Reactivity of Gaseous Glycine and its Derivatives. *Int. J. Mass Spectrom.* **2000,** *201,* 69–85.
30. Frisch, M. J.; Trucks, G. W.; Schlegel, H. B.; Scuseria, G. E.; Robb, M. A.; Cheeseman, J. R.; Zakrzewski, V. G.; Montgomery, J. A. Jr.;; Stratmann, R. E.; Burant, J. C.; Dapprich, S.; Millam, J. M.; Daniels, A. D.; Kudin, K. N.; Strain, M. C.; Farkas, O.; Tomasi, J.; Barone, V.; Cossi, M.; Cammi, R.; Mennucci, B.; Pomelli, C.; Adamo, C.; Clifford, S.; Ochterski, J.; Petersson, G. A.; Ayala, P. Y.; Cui, Q.; Morokuma, K.; Malick, D. K.; Rabuck, A. D.; Raghavachari, K.; Foresman, J. B.; Cioslowski, J.; Ortiz, J. V.; Baboul, A. G.; Stefanov, B. B.; Liu, G.; Liashenko, A.; Piskorz, P.; Komaromi, I.; Gomperts, R.; Martin, R. L.; Fox, D. J.; Keith, T.; Al-Laham, M. A.; Peng, C. Y.; Nanayakkara, A.; Gonzalez, C.; Challacombe, M.; Gill, P. M. W.; Johnson, B.; Chen, W.; Wong, M. W.; Andres, J. L.; Gonzalez, C.; Head-Gordon, M.; Replogle, E. S.; Pople, J. A. *Gaussian 98, Revision A7.* Gaussian, Inc.: Pittsburgh, PA, 1998.
31. Foster, J. P.; Weinhold, F. Natural Hybrid Orbitals. *J. Am. Chem. Soc.* **1980,** *102,* 7211–7218.
32. Glendening, E. D. Reed, A. E. Carpenter, J. E. Weinhold, F. *NBO Program, Version 3.1.*
33. Paizs, B.; Suhai, S. Combined Quantum Chemical and RRKM Modeling of the Main Fragmentation Pathways of Protonated GGG. I. Cis-trans Isomerization Around Protonated Amide Bonds. *Rapid Commun. Mass Spectrom.* **2001,** *15,* 2307–2323.
34. Uggerud, E. The Unimolecular Chemistry of Protonated Glycine and the Proton Affinity of Glycine: A Computational Model. *Theor. Chem. Acc.* **1997,** *97,* 313–316.